J. Phys. Chem. A **2001,** *105,* 6695−6702

Outer-Valence Green's Function Study of Cycloalkane and Cycloalkyl−Alkane Compounds

M. S. Deleuze*

Theoretische Scheikunde, Departement SBG, Limburgs Universitair Centrum, Universitaire Campus,
B3590 Diepenbeek, Belgium

J. Delhalle

Laboratoire Interdisciplinaire de Spectroscopie Electronique, Facultés Universitaires Notre-Dame de la Paix,
rue de Bruxelles 61, B5000 Namur, Belgium

Received: December 7, 2000; In Final Form: April 9, 2001

In this contribution, we report a quantitative analysis of gas-phase ultraviolet photoelectron spectra (HeI) of model compounds such as cyclopentane, cyclohexane, and cycloalkyl−1-alkane derivatives, by means of outer-valence Green's function (OVGF) calculations. These spectra and their OVGF theoretical simulations are also compared with UPS measurements on α-cycloalkyl−ω-alkanethiol monolayers adsorbed on gold. This theoretical study analyses the dependence of valence ionization spectra of saturated hydrocarbons on structural characteristics (configuration, conformation, and torsional flexibility).

1. Introduction

Thoroughly controlled fabrication of highly defined ultrathin organic layers is crucial for advanced technologies such as microelectronics and sensors. The optimization of the properties of such systems requires a sound knowledge of their surface molecular structure and of the orientation of the active elements. Owing to their very small sampling depth, electron spectroscopies enable direct and highly specific insight into the quantitative elemental composition and chemical bonding at the extreme surface of polymer materials and within organic thin films. Photoelectron spectroscopies are thus routinely used to obtain information on the chemical composition and homogeneity of organic surfaces but more rarely to extract information on their molecular structure. However, combined experimental and theoretical studies[1−7] have over the years provided consistent evidence of direct relationships between the molecular and the valence electronic structures.

In particular, several theoretical studies on saturated hydrocarbons in organic films and in the gas phase have amply demonstrated that valence photoemission spectra very finely fingerprint elements of their molecular architecture.[8−15] For instance, rather striking variations among the X-ray photoemission spectra (XPS) of large alkane chains[9−13] or cycloalkane compounds[14] have been predicted for subtle alterations of the molecular conformation, such as a chain folding,[9,10] ring inversion,[10] or the helicoidal distortion of isotactic polypropylene.[15] The potential of ultraviolet photoemission spectroscopy (UPS) in disclosing information on the molecular conformation has been also extensively assessed by measurements in the gas phase on compounds with electron lone pairs developing sufficiently strong nonbonding interactions,[16−18] as well as in detailed studies of the orientation and order of several organic thin films.[19−23] If XPS covers the whole valence band, it is surpassed in resolution by UPS, which gives rise in addition to larger cross sections in the outer-valence region.

In continuation of the above-mentioned works,[8−15] the present study aims at determining the type of structural information that can be accessible from a theoretical analysis of the UPS valence spectra of saturated hydrocarbons in the solid and gas phases, using the outer-valence Green's function approach.[24] With this purpose, we first consider high-resolution UPS (HeI) measurements on cyclopentane and cyclohexane[25] in the gas phase to evaluate the impact on such spectra of the cyclic connectivities and, in the case of cyclohexane, of ring inversion. We then address the case of recent gas-phase UPS (HeI) measurements[26] on cycloalkyl−1-alkane derivatives and on self-assembled monolayers (SAMs) of alkanethiols obtained by grafting 1-cyclohexyl−12-dodecanethiol ($C_6H_{11}(CH_2)_{12}SH$) and 1-cyclopentyl−12-dodecanethiol ($C_5H_9(CH_2)_{12}SH$) on gold. From their well-defined composition, thickness, and molecular structure,[27] these monolayers provide particularly attractive reference samples. From the synthetic and technological viewpoints, their main advantages are the straightforwardness of their preparation and their great chemical stability, due to the strong bonding between the sulfur and the metal surface. These alkanethiol molecules are chemically very similar—they are merely saturated hydrocarbon chains—but differ in their primary (configuration) and, depending on the environment, secondary (conformation) structures. These monolayers have also been characterized[28] by contact angle measurements, ellipsometry, IRAS, electrochemical measurements, and photoemission with synchrotron radiation. The motivation for a detailed analysis of the He(I) UPS spectra of these monolayers by comparison with He(I) measurements in the gas phase and accurate calculations of the electron binding energies of smaller model cycloalkyl−alkane compounds reside not only in the higher resolution achieved with gas-phase He(I) ultraviolet photoemission spectroscopy, but also in the straightforward distinction of the intramolecular characteristics (in particular vibrational broadening) from the intermolecular interactions and other solid-state effects.

2. Computations

Quantitative theoretical calculations based on the outer-valence Green's function approach (OVGF)[24] are used in the form of convoluted densities of states (DOS) for the following compounds: cyclopentane, cyclopentylmethane, cyclopentyle-

---

* Corresponding author. E-mail: deleuze@luc.ac.be.

10.1021/jp004406+ CCC: $20.00

thane, cyclohexane, cyclohexylmethane, cyclohexylethane, cyclohexyl−1-propane, and cyclohexyl−1-butane, in order to support the interpretation of outer-valence He(I) ionization spectra measured in the gas phase. This one-particle Green's function (1p-GF) approach enables a renormalized treatment of ionization energies, which is correct through the third order in the electron correlation potential, with the restriction of a diagonal Green's function and self-energy. As its name implies, this scheme is thus particularly well-suited for studies of one-electron outer-valence ionization processes. When there are no close-by excited (shake-up) states, an accuracy of typically 0.2−0.3 eV can be obtained for the one-electron binding energies, provided that a sufficiently large basis is used. In this work, we rely on the standard split-valence polarized 6-31G** basis set, with the exception of the OVGF calculations on the cyclohexyl−1-heptane [$C_6H_{11}-(CH_2)_6-CH_3$] and cyclopentyl−1-octane [$C_5H_9-(CH_2)_7-CH_3$] compounds which were used to model the alkanethiol monolayers and for which we restricted ourselves to a split-valence 6-31G basis only. From recent works on the ionization spectra of polyethylene,[29] carried out using a second-order and diagonal Green's function, as well as comparable but earlier works on oligomer series converging on this stereoregular polymer,[13,30] we assume nonetheless that the $C_6H_{11}-(CH_2)_6-CH_3$ and [$C_5H_9-(CH_2)_7-CH_3$] model molecules are large enough to compensate for the limitation of the latter basis by the contribution of a large number of atoms. In any case, since the work function of alkanethiol compounds is not known, we did not seek in this work the computationally demanding calculation of very accurate ionization energies of large alkanethiol chains, which in their adsorbed state display usually very little symmetry, or even no symmetry at all. To simplify the OVGF calculations, we have used the assumption of frozen core electrons.

These calculations have been carried out using the GAUSSIAN94 package of programs[31] on the ground of geometries optimized at the Hartree−Fock level with a 6-31G** basis set. Details of these geometries are illustrated for the cycloalkyl−alkane compounds considered in this work through the interplay of Figure 1**.** In all cases, the cyclohexyl− and cyclopentyl− fragments were given a chair and envelope conformation, respectively, whereas a zigzag planar conformation has been considered for the *n*-alkyl fragments. In the case of cyclopentane, both the nearly isoenergetic envelope (C_s) and half-chair (C_2) forms[14] have been considered. In addition to the largely prevailing chair (D_{3d}) conformer of cyclohexane, we also consider the boat (C_{2v}) and twisted-boat (D_2) forms,[14] corresponding at the HF/6-31G** level to first-order saddle points and local energy minima at 7.85 and 6.78 kcal mol^{-1} above the chair form, respectively, to evaluate the impact of ring inversion on the outer valence ionization energies.

No cross section effects are accounted for in the present calculations. The spread function used to convolute the OVGF ionization spectra of cycloalkyl−alkanes has been taken as a linear combination of one Gaussian and one Lorentzian with equal weight and width (in general, fwhm = 0.9 eV), to roughly account for experimental resolution and vibrational broadening. With regard to the average He(I) line width observed within Kimura measurements[25] on saturated hydrocarbons, the ionization spectra of cyclopentane and cyclohexane have been simulated assuming a fwhm parameter of 0.4 eV.

The interested reader is referred to refs 32−35 for even more involved Green's function and large basis set treatments of the ionization spectra of saturated hydrocarbons, which in particular fully account for the dispersion of ionization intensity into shake-up processes. For such compounds, the onset of the shake-up contamination lies at an ionization energy of about 23 eV,[32,33] i.e., far beyond the electron binding energy range which is the subject of this study. From a comparison of 6-31G** results[32] with a particularly thorough 6-311++G** study of the ionization spectrum of *n*-butane,[34] one can reasonably assume that the 6-31G** one-electron binding energies presented here should not deviate in average by more than 0.1 eV from their complete basis set limit. Compared with the exact (full-CI) value, an overall accuracy of 0.3 eV can thus be expected.

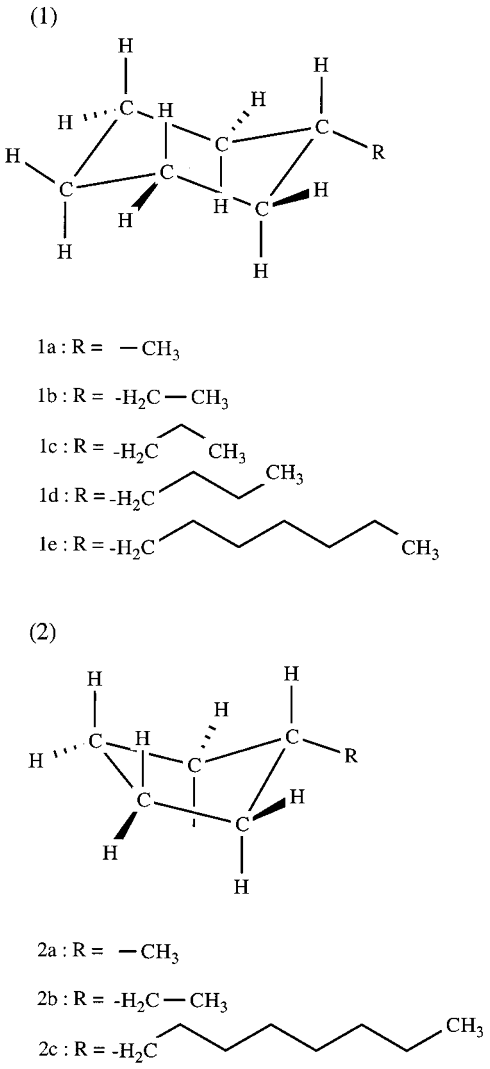

Figure 1. Model molecular structures considered in this work.

It should be stressed that binding energies in the gas-phase measurements are referenced to the vacuum level, whereas the binding energies in the experimental UPS solid-phase spectra were referenced to the Fermi level of gold.

3. Results and Discussion

Gas-Phase UPS Spectra of Cyclopentane and Cyclohexane. High-resolution He(I) records[25] on cyclopentane and cyclohexane are reproduced in Figures 2a and 3a and can be readily compared with the OVGF spectra displayed in Figures 2b,c and 3b−d for the selected forms of these compounds.

The He(I) photoionization spectrum of cyclopentane (Figure 2a) exhibits four well-resolved peaks, with maxima at binding energies of 11.8, 14.2, 16.0, and ~18.6 eV, in quantitative agreement with the energy location of the four peaks that appear

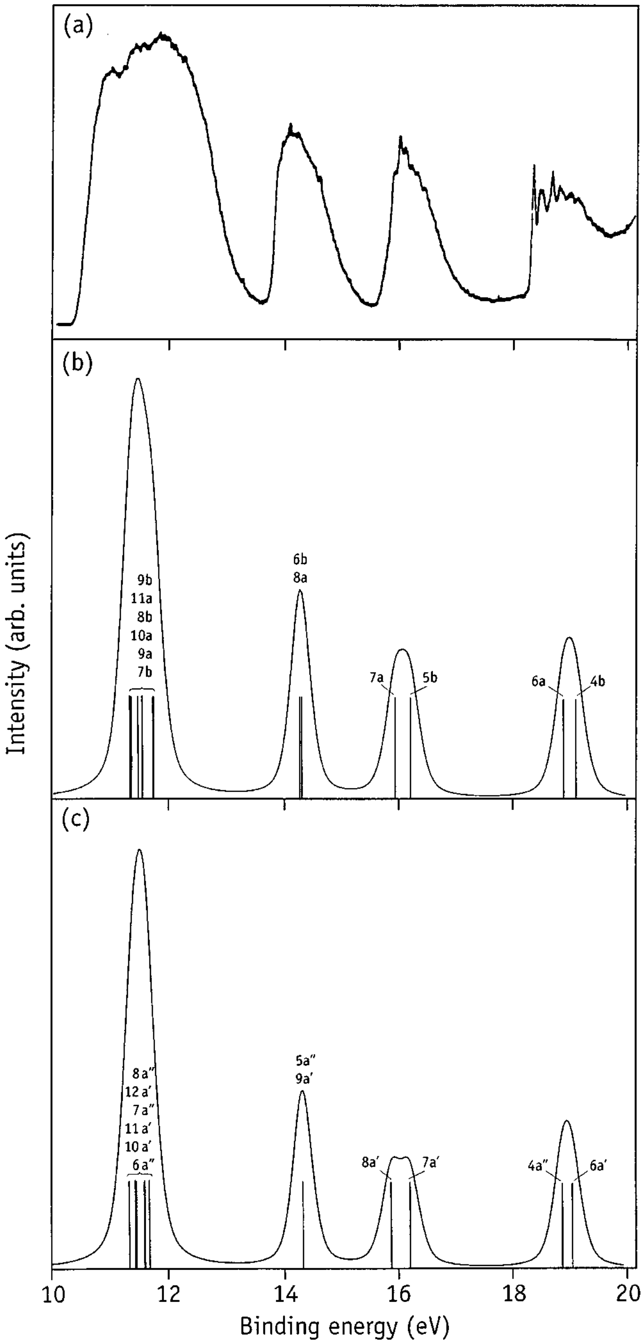

Figure 2. Comparison of the gas-phase UPS (HeI) spectrum[25] of cyclopentane (a) with OVGF simulations (fwhm = 0.4 eV) for the envelope (b) and half-chair (c) forms of this compound.

in the OVGF simulations (Figure 2b,c) at 11.5, 14.3, 16.1, and 19.0 eV. This clear separation of ionization lines is the direct outcome of the five-membered cyclic connectivity. When the low-energy lying planar D_{5h} transition state that connects the envelope and chair forms of this very floppy molecule is considered, the six outermost one-electron energy levels fall in three degenerate pairs ($3e_2'$, $3e_1'$, and $1e_2''$) within an energy interval less than 0.3 eV.[14] Similarly, the two nearly degenerate ionization lines at 14.3 eV correlate with the $1e_1''$ doubly degenerate one-electron level of the planar D_{5h} form. The degeneracy of these outer-valence levels is removed only by a few hundredths of an electronvolt when cyclopentane lies in its envelope or half-chair conformation.[14] On the other hand, symmetry lowering from the planar D_{5h} form appears to have

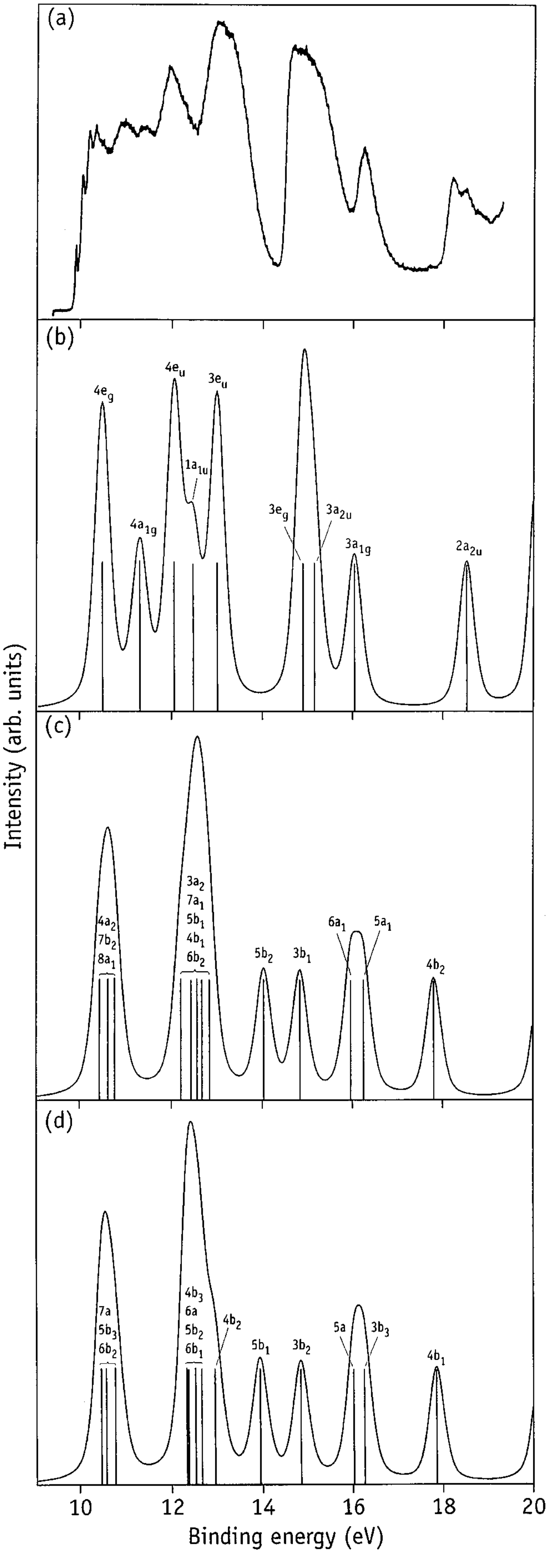

Figure 3. Comparison of the gas-phase UPS (HeI) spectrum[25] of cyclohexane (a) with OVGF simulations (fwhm = 0.4 eV) for the chair (b), boat (c), and twisted-boat (d) forms of this compound.

TABLE 1: Experimental[25] (gas-phase UPS HeI) vs OVGF/6-31G One-Electron Binding Energies (in eV) of Cyclopentane (pole strengths in brackets)**

level			exptl.	theory			
				half-chair (C_2)		envelope (C_s)	
MO[a]	character[b]	bonding[c]	He(I)	MO	IP (Γ)	MO	IP (Γ)
15	$C_{2p} + H_{1s}$	C−H	11.01	$8a''$	11.346 (0.921)	9b	11.438 (0.922)
14	$C_{2p} + H_{1s}$	C−H	11.39	$12a'$	11.561 (0.921)	11a	11.336 (0.912)
13	$C_{2p} + H_{1s}$	C−C	11.82	$7a''$	11.371 (0.912)	8b	11.461 (0.912)
12	$C_{2p} + H_{1s}$	C−C	11.82	$11a'$	11.488 (0.912)	10a	11.683 (0.921)
11	$C_{2p} + H_{1s}$	C−C/C−H	12.0	$10a'$	11.743 (0.914)	9a	11.607 (0.914)
10	$C_{2p} + H_{1s}$	C−C/C−H	12.0	$6a''$	11.757 (0.914)	7b	11.597 (0.913)
9	$C_{2p} + H_{1s}$	C−H	14.21	$5a''$	14.290 (0.913)	6b	14.346 (0.913)
8	$C_{2p} + H_{1s}$	C−H	14.21	$9a'$	14.324 (0.913)	8a	14.349 (0.913)
7	$C_{2p} + H_{1s}$	C−H	15.96	$8a'$	15.951 (0.906)	7a	15.894 (0.906)
6	$C_{2p} + H_{1s}$	C−H	16.5	$7a'$	16.214 (0.909)	5b	16.219 (0.909)
5	C_{2s}	C−H/C−C		$4a''$	18.897 (0.891)	6a	18.896 (0.891)
4	C_{2s}	C−H/C−C		$6a'$	19.111 (0.891)	4b	19.072 (0.891)
3	C_{2s}	C−C		$5a'$	23.017 (0.857)	5a	23.015 (0.856)
2	C_{2s}	C−C		$3a''$	23.030 (0.857)	3b	23.027 (0.857)
1[d]	C_{2s}	C−C		$4a'$	26.426 (0.813)	4a	26.380 (0.813)

[a] HF orbital energy order. [b] Evaluated from the dominant AO type. [c] Dominant bonding pattern, qualitatively evaluated from a visualization of the molecular orbitals of the C_s form. [d] Inner-valence level subject to a severe breakdown of the orbital picture of ionization (see ref 32).

TABLE 2: Experimental[25] (gas-phase UPS HeI) vs OVGF/6-31G One-Electron Binding Energies (in eV) of Cyclohexane (pole strengths in brackets)**

level			exptl.	theory					
				chair (D_{3d})		boat (C_{2v})		twisted-boat (D_2)	
MO[a]	type[b]	bonding[c]	(HeI)	MO	IP (Γ)	MO	IP (Γ)	MO	IP (Γ)
18	$C_{2p} + H_{1s}$	C−C/C−H	10.32	$4e_g$	10.459 (0.914)	$4a_2$	10.407 (0.914)	7a	10.449 (0.914)
17	$C_{2p} + H_{1s}$	C−C/C−H	10.93	″	″	$7b_2$	10.743 (0.921)	$5b_3$	10.559 (0.916)
16	$C_{2p} + H_{1s}$	C−H	11.38	$4a_{1g}$	11.278 (0.923)	$8a_1$	10.594 (0.915)	$6b_2$	10.757 (0.921)
15	$C_{2p} + H_{1s}$	C−H	11.90	$4e_u$	12.027 (0.917)	$3a_2$	12.191 (0.917)	$4b_3$	12.313 (0.917)
14	$C_{2p} + H_{1s}$	C−H	″	″	″	$7a_1$	12.549 (0.917)	6a	12.507 (0.917)
13	$C_{2p} + H_{1s}$	C−C	12.94	$1a_{1u}$	12.448 (0.904)	$5b_1$	12.414 (0.907)	$5b_2$	12.351 (0.906)
12	$C_{2p} + H_{1s}$	C−C/C−H	12.94	$3e_u$	12.984 (0.912)	$4b_1$	12.662 (0.909)	$6b_1$	12.645 (0.911)
11	$C_{2p} + H_{1s}$	C−C/C−H	″	″	″	$6b_2$	12.830 (0.912)	$4b_2$	12.941 (0.911)
10	$C_{2p} + H_{1s}$	C−H	14.62	$3e_g$	14.886 (0.910)	$5b_2$	14.036 (0.913)	$5b_1$	13.943 (0.913)
9	$C_{2p} + H_{1s}$	C−H	″	″	″	$3b_1$	14.834 (0.910)	$3b_2$	14.837 (0.910)
8	$C_{2p} + H_{1s}$	C−H	14.62	$3a_{2u}$	15.140 (0.912)	$6a_1$	15.963 (0.906)	5a	16.011 (0.906)
7	$C_{2p} + H_{1s}$	C−H	16.15	$3a_{1g}$	16.032 (0.906)	$5a_1$	16.249 (0.908)	$3b_3$	16.251 (0.907)
6	C_{2s}	C−H		$2a_{2u}$	18.521 (0.896)	$4b_2$	17.812 (0.898)	$4b_1$	17.849 (0.898)
5	C_{2s}	C−C/C−H		$2e_g$	20.122 (0.880)	$2a_2$	20.198 (0.880)	4a	20.157 (0.880)
4	C_{2s}	C−C/C−H		″	″	$4a_1$	20.373 (0.880)	$2b_3$	20.404 (0.880)
3	C_{2s}	C−C		$2e_u$	23.926 (0.849)	$2b_1$	23.786 (0.848)	$3b_1$	23.811 (0.849)
2	C_{2s}	C−C		″	″	$3b_2$	23.901 (0.849)	$2b_2$	23.847 (0.849)
1[d]	C_{2s}	C−C		$2a_{1g}$	26.385 (0.819)	$3a_1$	26.273 (0.814)	3a	23.847 (0.815)

[a] HF orbital energy order. [b] Evaluated from the dominant AO type. [c] Dominant bonding pattern, qualitatively evaluated from a visualization of the molecular orbitals of the D_{3d} form. [d] Inner-valence level subject to a severe breakdown of the orbital picture of ionization (see ref 32).

a stronger effect on the highest inner-valence (C_{2s}) $2e_2'$ electron level. Specifically, the double degenaracy of this level is released by ∼0.2 eV when cyclopentane resides in its half-chair or envelope conformation. Except for marginal variations by a few hundredths of an electronvolt in bandwidths, the OVGF spectra simulated for the envelope and chair forms of cyclopentane are practically identical.

With regard to the many energy degeneracies and near-degeneracies which characterize its valence electronic structure, cyclopentane must certainly be subject to particularly intense Jahn−Teller distortions and vibronic interactions during ionization, in particular when tackling one of the six outermost levels encompassed within the peak at ∼11.8 eV. Actually, this peak is found experimentally (Figure 2a) to be very strongly broadened (fwhm = 2.2 eV), in sharp contrast with the theoretical results (fwhm = 0.7 eV) based on a vertical picture of ionization (Figure 2b,c). This discrepancy must evidently be interpreted[10] as the outcome of strong vibronic coupling effects due to ionization, which very likely evolve into fast rotating vibrations (rotons) in the molecular cation. Similarly, substantial broadening can be seen in the He(I) spectrum (Figure 2a) for the peaks at 14.2 and ∼18.4 eV, relating to the $1e_1''$ and $2e_2'$ pairs of the planar D_{5h} form. In the latter case, nice vibrational progressions, starting at ∼11.2 and ∼11.6 eV, can even be noticed.

Unlike cyclopentane, the OVGF simulations for cyclohexane (Figure 3b−d) indicate that ring inversion from the chair to the higher energy-lying boat or twisted-boat form would have an easily recognizable impact on high-resolution He(I) spectra. The theoretical OVGF spectrum of the chair form (Figure 3b) exhibits six well-resolved peaks in the outer-valence region, at 10.5 ($4e_g$), 11.3 ($4a_{1g}$), 12.0 ($4e_u$), 13.0 ($3e_u$), 14.9 ($3e_g + 3a_{2u}$), and 16.0 eV ($3a_{1g}$), overall in quantitative agreement (Table 2) with the energy locations of the peaks seen in the available He(I) spectrum (Figure 3a). In addition, an asymmetric vibrational progression starting at 18.2 eV can be related to the highest inner-valence ($2a_{2u}$) level, for which our OVGF/6-31G** calculations give a vertical ionization energy of 18.5 eV. The

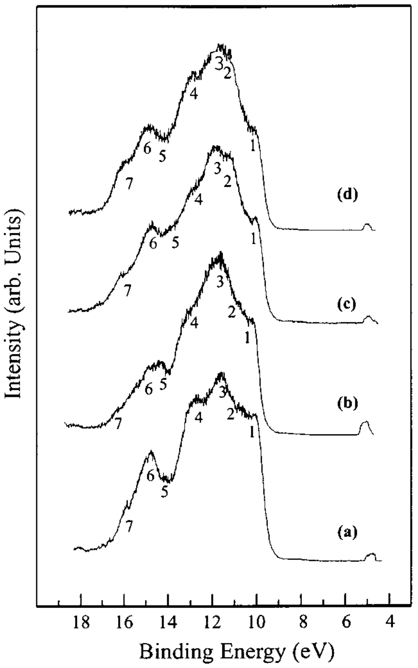

Figure 4. Gas-phase UPS (HeI) spectra[26] of cyclohexylmethane (a), cyclohexylethane (b), cyclohexyl−1-propane (c), and cyclohexyl−1-butane (d).

intense peak at about 14.9 eV is the very typical spectral signature for the $C_{2s}-C_{2p}$ orbital mixing[12,13] due to annular methylenic hyperconjugation,[10−15] which the chair form of cyclohexane permits.

Most generally, band intensities in the He(I) spectrum (Figure 3a) closely follow the orbital multiplicities imposed by the D_{3d} symmetry of the chair form of cyclohexane. One striking exception occurs with the outermost $4e_g$ level, which appears experimentally in the form of two vibrational progressions with equal intensity and maxima at ionization energies of 10.3 and 10.9 eV. Here also, this discrepancy with the OVGF results is certainly the outcome of vibronic interactions initiated by a Jahn−Teller distortion.

In sharp contrast with the results of the OVGF simulation for the chair form (Figure 3b), the eight outermost ionization lines of the boat (Figure 3c) and twisted-boat (Figure 3d) forms of cyclohexane fall within two sharp and very intense peaks, near binding energies of ∼10.6 and ∼12.4 eV. Also of relevance for the present work is the splitting of the ($3e_g + 3a_{2u}$) orbital "triplet" of the chair confomer over three well-resolved ionization lines at 10.0, 14.8, and 16.0 eV with the boat and twisted-boat forms. This results in clear variations of band shapes and intensities that directly reflect different through-space interactions between neighboring methylenic C−H bonds. At last, ring inversion from the chair form yields a substantial destabilization, from 18.5 to 17.8 eV, of the energy level at the top of the inner-valence region ($2a_{2u}$, or $6a_1$ or 5a in the boat or twisted-boat form). This also directly relates[14] to the slackening of through-space methylenic hyperconjugation.

Gas-Phase UPS Spectra of Cycloalkyl−Alkane Compounds. The UPS gas-phase spectra[26] of four cyclohexylalkane compounds are shown in Figure 4 and can be readily compared with the OVGF simulations displayed for these compounds in Figure 5. Details of the comparison are given in Table 3. Three peaks, labeled 1, 3, and 6, dominantly and systematically emerge from the He(I) outer-valence bands at binding energies of about 10.0, 11.5, and 14.8 eV. In the OVGF simulations, the sharpest and best-resolved peaks are correspondingly located at 10.0, 11.5, and 14.7 eV, thus in quite remarkable agreement with experiment. Substructures, labeled 2, 4, 5, and 7 are also seen at ∼10.5, 12.8, 14.2, and 16.0 eV in the He(I) spectra, which correlate (Table 3) quite nicely with marginal peaks at comparable binding energies in the OVGF spectra.

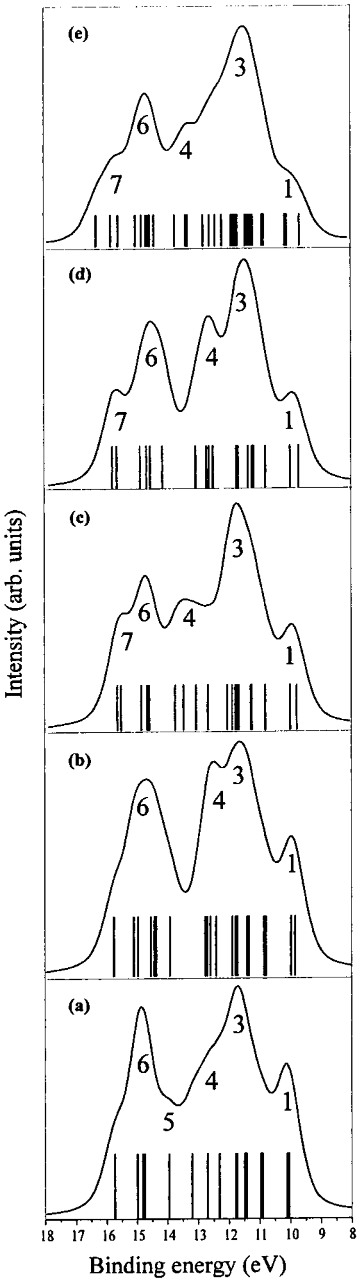

Figure 5. Theoretical (OVGF) ionization spectra (fwhm = 0.9 eV) of cyclohexylmethane (a), cyclohexylethane (b), cyclohexyl−1-propane (c), cyclohexyl−1-butane (d), and cyclohexyl−1-heptane (e).

The well-marked peak (6) at about 14.8 eV is here also the very typical spectral signature for the annular methylenic hyperconjugation which prevails within a cyclohexyl ring lying in chair conformation. By extrapolation of the results obtained previously for cyclohexane, it is clear that ring inversion to the boat form would result into a splitting of this peak to the gathering of the outermost ionization lines into two sets centered at ∼10.6 and ∼12.4 eV and, thus, overall to a very different outer valence signal. The increase of the chain length grafted to the ring results in a progressive smoothing of the features from the ring, notably the structure around 10 eV (Figure 5a−e). Nonetheless, despite large densities of states, the OVGF

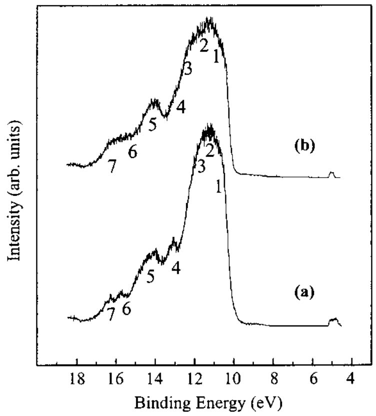

Figure 6. Gas-phase UPS (HeI) spectra[26] of cyclopentylmethane (a) and cyclopentylethane (b).

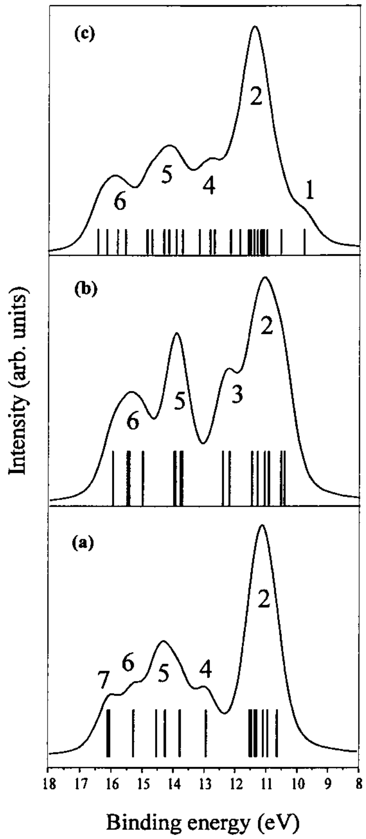

Figure 7. Theoretical (OVGF) ionization spectra (fwhm = 0.9 eV) of cyclopentylmethane (a), 1-cyclopentylethane (b), and cyclopentyl−1-octane (c).

TABLE 3: Experimental[26] (gas-phase UPS HeI) and Theoretical (OVGF/6-31G) Electron Binding Energies (in eV) of the Cycloalkyl−Alkane Compounds Considered in This Work**

molecule	peak	UPS results position	theoretical results position	theoretical results relative intensity (%)
cyclohexylmethane	1	10.0	10.1	66.2
	2	10.5	–	–
	3	11.7	11.7	100.0
	4	12.8	12.7	70.8
	5	14.2	13.9	51.6
	6	14.8	14.8	91.5
	7	16.0	–	–
cyclohexylethane	1	10.0	10.0	59.0
	2	10.5	–	–
	3	11.7	11.6	100.0
	4	12.8	12.5	91.8
	5	14.2	–	–
	6	14.8	14.6	84.5
	7	16.2	–	–
cyclohexyl−1-propane	1	10.0	9.9	46.0
	2	11.2	–	–
	3	11.9	11.7	100.0
	4	12.8	13.4	57.9
	5	14.0	–	–
	6	14.8	14.7	68.6
	7	16.0	15.4	51.9
cyclohexyl−1-butane	1	10.0	9.9	41.5
	2	11.0		100.0
	3	11.5	11.5	–
	4	12.8	12.6	75.5
	5	–	–	–
	6	14.8	14.6	73.6
	7	16.0	15.7	44.0
cyclopentylmethane	1	10.8	–	–
	2	11.1	11.1	100.0
	3	12.1	–	–
	4	13.0	13.0	30.4
	5	14.0	14.3	50.2
	6	15.8	15.3	31.5
	7	16.2	16.0	27.2
cyclopentylethane	1	10.8	–	–
	2	11.1	11.1	100.0
	3	12.2	12.2	60.1
	4	–	–	–
	5	14.0	13.9	75.8
	6	15.8	15.4	50.0
	7	16.2	–	–

simulation for the 1-cyclohexyl−1-heptane compound (Figure 5e) confirm that the spectral features labeled 1, 3, and 6 which characteristically fingerprint the cyclohexyl ring in chair conformation are still easily recognizable, even when a large alkyl group is attached to it and despite the lower resolution of the gas-phase He(I) spectra displayed in ref 26.

Three well-resolved structures are seen at ~11, 14, and 16 eV within the UPS (HeI) spectra (Figure 6) of cyclopentylmethane and cyclopentylethane. The structure centered around 11 eV encompasses at least three substructures (1−3) at about 10.8, 11.1, and 12.1 eV. The structure observed at ~16 eV is made of two peaks (6 and 7), situated at 15.8 and 16.2 eV. The He(I) spectrum (Figure 6a) of the cyclopentylmethane compound exhibits a peak (labeled 4) at 13.0 eV, which seems to correlate with a shoulder in the He(I) spectrum (Figure 6b) of the cyclopentylethane molecule. The OVGF spectra simulated for these compounds (Figure 7) display two largely dominating structures, labeled 2 and 5, at binding energies of 11.1 eV and ~14 eV, in excellent agreement with experiment (Table 3). The substructures labeled 4, 6, and 7, which emerge at binding energies of 13.0, 15.3, and 16.0 eV from the theoretical spectrum of the cyclopentylmethane compound (Figure 7a), also very satisfactory correlate with the He(I) records on this compound. Only two peaks (5 and 6) are clearly resolved above 12.5 eV in the OVGF simulation for the cyclopentylethane molecule (Figure 7b), which is qualitatively in line with the He(I) measurement on this compound. On the other hand, no ionization line is found in this case at 13.0 eV, at odds with the shoulder seen experimentally (4 in Figure 6b) at this binding energy.

Despite the lower experimental resolution and the mixing with the electronic states relating to the methyl group, the outermost peak (around 11 eV) of cyclopentylmethane (Figure 6a) is much more intense and significantly sharper (fwhm = 2.0 eV) than the one observed in the He(I) spectrum[25] (fwhm = 2.2 eV) or in the XPS spectrum[10] (fwhm = 2.5 eV) of cyclopentane alone. The experimental width for this peak is also in qualitative

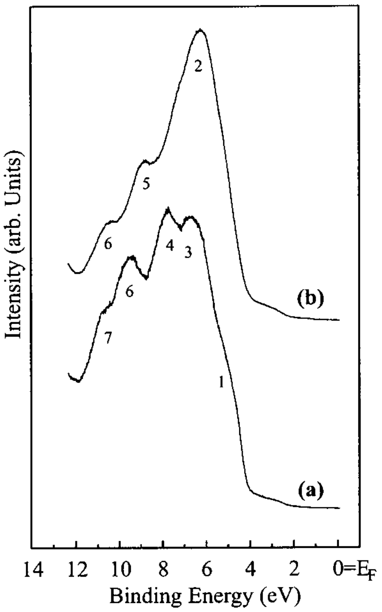

Figure 8. UPS (HeI) spectra recorded[26] with a TOA of 20° from 1-cyclohexyl−12-dodecanethiol (a) and 1-cyclopentyl−12-dodecanethiol (b) monolayers adsorbed on annealed Au/Si substrates.

agreement with the one (fwhm = 1.5 eV) predicted from the OVGF simulation. It should be stressed that this very significant difference between the He(I) measurements[26] on cycloalkyl derivatives and the He(I)[25] and XPS[10] measurements on cyclopentane cannot be accounted for by differences in resolutions between the photoelectron spectrometers used to complete the measurements reported in refs 25, 26, and 10 (0.03, 0.15, and 0.45 eV, respectively). It thus appears that the methyl group attached to the cyclopentyl ring is probably sufficient by itself to strongly inhibit vibronic interactions and their transformation into rotating vibrations. The increase in the width of the outermost peak (fwhm = 2.8 eV) in the He(I) spectrum of cyclopentylethane (Figure 6b) is qualitatively supported by a larger spreading (fwhm = 2.0 eV) of the ionization band (2) at 11.1 eV in the OVGF spectrum (Figure 7b), supporting the suggestion that broadening in this case is essentially and simply due to the influence on the valence electronic structure of a larger alkyl substituent, leading to a larger spreading in energy of outer-valence orbitals. According to the OVGF results, this band is found to evolve back to a slightly sharper peak (fwhm = 1.8 eV) when the length of the alkyl substituent increases (Figure 7c). A shift at slightly larger binding energies (11.3 eV) is also noted. Despite band broadening due to the energy spreading of the outer-valence band system and with regard to the OVGF simulations previously displayed (Figure 2b,c) for cyclopentane, the presence of a very sharp and intense peak at 11.3 eV in the OVGF theoretical spectrum of the cyclopentyl−1-octane compound (Figure 7c) is the most obvious spectral feature for the cyclopentyl moiety.

Solid-Phase UPS Spectra of Monolayers. HeI spectra of the cyclohexyl−12-dodecanethiol and cyclopentyl−12-dodecanethiol monolayers obtained on annealed Au/Si slides[26] are shown in Figure 8 and characterized against the OVGF results reported for the cyclohexyl−1-heptane and cyclopentyl−1-octane model molecules in Table 4. The UPS spectrum of cyclohexyl−12-dodecanethiol (Figure 8a) is composed of a shoulder around 4.8 eV and two pairs of peaks separated by a significant depletion of ionization intensity at about 8.7 eV. In regard with the work function of the substrate, the peak (6) found at 9.5 eV correlates with the peak (6) which is systematically seen at 14.8 eV in the gas-phase He(I) spectra of the cyclohexylmethane, -ethane, -1-propane and -1-butane compounds (Figure 4). This peak and the overall shape of the outer-valence band confirm therefore that the cyclohexane rings in the monolayers still remain in the chair conformation,[14] despite packing and disorder effects.[28] The consistency of our analysis is further supported by a very satisfactory agreement overall between these solid-phase measurements and the OVGF/6-31G spectrum (Figure 5e) simulated for the cyclohexyl−1-heptane compound.

TABLE 4: Comparison of the Experimental (solid-phase UPS HeI) Electron Binding Energies (in eV) of the α-Cycloalkyl−ω-alkanethiol Monolayers[26] Considered in This Work to the Theoretical (OVGF/6-31G) One-Electron Ionization Energies of Model Cycloalkyl−alkane Compounds

			theoretical results	
molecule	peak	UPS results position	position	relative intensity (%)
1-cyclohexyl−12-dodecanethiol (UPS results) and heptylcyclohexane (theoretical results)	1	4.8	10.0	34.4
	2	−	−	−
	3	6.6	11.4	100.0
	4	7.7	13.2	56.3
	5	−	−	−
	6	9.5	14.7	70.0
	7	10.8	15.6	42.2
1-cyclopentyl−12-dodecanethiol (UPS results) and octylcyclopentane (theoretical results)	1	−	9.8	19.2
	2	−	−	−
	3	6.2	11.3	100.0
	4	−	12.7	42.3
	5	−	−	−
	6	8.8	14.1	48.4
	7	10.5	15.8	35.1

The shape of the outer valence band in the UPS spectrum of the 1-cyclopentyl−12-dodecanethiol monolayer (Figure 8b) can also be qualitatively compared with the OVGF/6-31G spectrum for the cyclopentyl−1-octane compound (Figure 7c). Here also, a rather sharp and intense peak is seen on the experimental side at the top of the outer valence region (at 6.2 eV). The qualitative agreement between the OVGF and He(I) bandwidths confirms that strong vibronic coupling effects are suppressed, or at least strongly impeded, because of the alkyl segment grafted to the gold substrate. The presence of the latter substituent on the ring obviously releases electronic degeneracies and also unfavorably affects the torsional (or, more precisely, pseudorotational) flexibility of the cyclopentyl moieties.

5. Concluding Remarks

In the present work, various gas-phase UPS measurements on cyclopentane, cyclohexane, and several cycloalkyl−1-alkane derivatives in the gas phase have been compared against the results of quantitative theoretical OVGF calculations, with the aim of evaluating the potential of photoelectron spectroscopies in elucidating the molecular structure of monolayers of alkanethiol compounds grafted on gold. The compounds that have been chosen for this purpose are chemically very similar but differ in their configuration and, possibly, in their conformation. In comparison with cyclopentane, cyclopentyl−1-alkane derivatives are also characterized by a higher rigidity. Our OVGF calculations confirm that UPS is highly sensitive to the primary structure of saturated hydrocarbon rings and chains, each giving rise to a typical fingerprint in the valence spectra. A comparison between theory and experiment undoubtedly demonstrates that the cyclohexyl rings remain in chair conformation in the case of the 1-cyclohexyl−12-dodecanethiol monolayer, as well as with the alkyl derivatives of cyclohexane. The excellent agreement between the He(I) and OVGF results also indicate that a grafted 1-cyclopentyl−12-dodecanethiol chain is not subject to particularly strong Jahn−Teller effects, as could be feared with regard to high-resolution He(I) measurements on cyclopentane. Very interestingly, because of the lack of obvious experimental evidence for strong vibronic coupling effects in the He(I) records, the presence of simply a methyl substituent appears also to significantly release electronic degeneracies and to strongly reduce the conformational flexibility of cyclopentane, thereby preventing very strong vibronic coupling effects even in the case of the cyclopentylmethane derivative.

Since the solid-phase UPS spectra of the α-cycloalkyl−ω-alkanethiol monolayers are very similar to the theoretical OVGF and gas-phase UPS spectra of the cycloalkyl−1-alkane model chains, one can conclude that the sulfur atom (S_{3p} at 8 eV with $E_F = 0$) does not contribute significantly to the UPS spectral features of the films. Furthermore, this similarity shows that SAMs of alkanethiols are good reference systems for the study of typical molecular structures.

A main conclusion of this study is that UPS measurements nowadays can provide access to detailed information on the molecular structure (configuration, conformation) when compared with the results of theoretical calculations coping accurately with electronic correlation and relaxation. Even when such calculations are based on the vertical picture of ionization, UPS measurements can also lead to indirect and qualitative insight into the conformational flexibility of the investigated compounds. However, more detailed calculations dealing properly with nuclear dynamics[36] are clearly required to clarify on quantitative grounds the impact of vibronic couplings on line broadening.

Acknowledgment. M.S.D. is grateful to the “Fonds voor Wetenschappelijk Onderzoek van Vlaanderen” and to the “Bijzonder OnderzoeksFonds” of the Limburgs Universitair Centrum for financial support. This work was supported in part by the Interuniversity Research Program in Reduced Dimensionality Systems (PAI/IUAP 4/10).

References and Notes

(1) Delhalle, J.; André, J.-M.; Delhalle, S.; Pireaux, J.-J.; Caudano, R.; Verbist, J. *J. Chem. Phys.* **1974**, *60*, 595.

(2) Pireaux, J.-J.; Riga, J.; Caudano, R.; Verbist, J. In *Photon, Electron and Ion Probes of Polymer Structure and Properties*; Dwight, D. W., Fabish, Th. J., Thomas, H. R., Eds.; ACS Symp. Series No 162; American Chemical Society: Washington, DC, 1981; p 169.

(3) Salaneck, W. R. In *CRC Critical Reviews in Solid State and Materials Science*; CRC Press: Cleveland, 1985; Vol. 12, pp 267−296 and references therein.

(4) Boulanger, P.; Lazzaroni, R.; Verbist, J.; Delhalle, J. *Chem. Phys. Lett.* **1986**, *129*, 275.

(5) Salaneck, W. R.; Brédas, J.-L. In *Organic Materials for Electronics*; Brédas, J.-L., Salaneck, W. R., Wegner, G., Eds.; North-Holland: Amsterdam, 1994; p 15.

(6) Yoshimura, D.; Ishii, H.; Ouchi, Y.; Ito, E.; Miyamae, T.; Hasegawa, S.; Okudaira, K. K.; Ueno, N.; Seki, K. *Phys. Rev. B* **1999**, *60*, 9046.

(7) Beamson, G.; Pickup, B. T.; Li, W.; Mai, S.-M. *J. Phys. Chem. B* **2000**, *104*, 2656.

(8) Delhalle, J.; Deleuze, M. *J. Mol. Struct. (THEOCHEM)* **1992**, *261*, 187.

(9) (a) Delhalle, J.; Denis, J. P.; Deleuze, M.; Riga, J.; Dosière, M. *Chem. Phys. Lett.* **1993**, *210*, 21. (b) Riga, J.; Delhalle, J.; Deleuze, M.; Pireaux, J. J.; Verbist, J. *Surf. Int. Anal.* **1994**, *22*, 507.

(10) Deleuze, M.; Delhalle, J.; Pickup, B. T.; Svensson, S. *J. Am. Chem. Soc.* **1994**, *116*, 10715.

(11) Delhalle, J.; Delhalle, S.; Riga, J. *J. Chem. Soc., Faraday Trans. 2* **1987**, *83*, 503.

(12) Deleuze, M.; Denis, J.-P.; Delhalle, J.; Pickup, B. T. *J. Phys. Chem.* **1993**, *97*, 5115.

(13) Deleuze, M.; Delhalle, J.; Pickup, B. T. *Chem. Phys.* **1993**, *175*, 427.

(14) Deleuze, M.; Delhalle, J.; Pickup, B. T. *J. Phys. Chem.* **1994**, *98*, 2382.

(15) Flamant, I.; Mosley, D. H.; Deleuze, M.; André, J.-M.; Delhalle, J. *Int. J. Quantum Chem.* **1994**, *S28*, 469.

(16) Guimon, M. F.; Guimon, C.; Metras, F.; Pfister-Guillouzo, G. *J. Am. Chem. Soc.* **1976**, *98*, 2078.

(17) Carnovale, F.; Gan, T. H.; Peel, J. B. *J. Electron Spectrosc. Relat. Phenom.* **1979**, *16*, 87.

(18) Karlsson, L.; Åsbrink, L.; Fridh, C.; Lindholm, E.; Svensson, A. *Phys. Scr.* **1980**, *21*, 170.

(19) Seki, K.; Ueno, N.; Karlsson, U. O.; Engelhardt, R.; Koch, E.-E. *Chem. Phys.* **1986**, *105*, 247.

(20) Seki, K.; Inokuchi, H. *Chem. Phys. Lett.* **1982**, *89*, 268.

(21) Seki, K.; Sato, N.; Inokuchi, H. *Chem. Phys.* **1993**, *178*, 207.

(22) Hasegawa, S.; Tanaka, S.; Yamashita, Y.; Inokuchi, H.; Fujimoto, H.; Kamiya, K.; Seki, K.; Ueno, N. *Phys. Rev. B* **1993**, *48*, 2596.

(23) Ueno, N. *Jpn. J. Appl. Phys.* **1999**, *38* (suppl. 1), 226.

(24) (a) Cederbaum, L. S. *Adv. Chem. Phys.* **1977**, *36*, 205. (b) von Niessen, W.; Schirmer, J.; Cederbaum, L. S. *Comput. Phys. Rep.* **1984**, *1*, 57. (c) Ortiz, J. V. *J. Chem. Phys.* **1988**, *89*, 6348. (d) Zakrzewski, V. G.; von Niessen, W. *J. Comput. Chem.* **1993**, *14*, 13.

(25) Kimura, K.; Katsumata, S.; Achiba, Y.; Yamazaki, T.; Iwata, S. *Handbook of HeI. Photoelectron Spectra of Fundamental Organic Molecules*; Halsted Press: New York, 1981.

(26) Duwez, A.-S.; Pfister-Guillouzo, G.; Delhalle, J.; Riga, J. *J. Phys. Chem. B* **2000**, *104*, 9029.

(27) Ulman, A. *Chem. Rev.* **1996**, *96*, 1533.

(28) (a) Duwez, A.-S.; Riga, J.; Ghijsen, J.; Pireaux, J.-J.; Verbist, J. J.; Delhalle, J. *J. Electron Spectrosc. Relat. Phenom.* **1995**, *76*, 523. (b) Duwez, A.-S.; Riga, J.; Han, B. Y.; Delhalle, J. *J. Electron Spectrosc. Relat. Phenom.* **1996**, *81*, 55. (c) Duwez, A.-S.; Di Paolo, S.; Ghijsen, J.; Riga, J.; Deleuze, M. S.; Delhalle, J. *J. Phys. Chem. B* **1997**, *101*, 884.

(29) Sun, J.-Q.; Bartlett, R. J. *Phys. Rev. Lett.* **1996**, *77*, 3669.

(30) Deleuze, M.; Delhalle, J.; Pickup, B. T. *J. Electron Spectrosc. Relat. Phenom.* **1992**, *60*, 37.

(31) Frisch, M. J.; Trucks, G. W.; Schlegel, H. B.; Gill, P. M. W.; Johnson, B. G.; Robb, M. A.; Cheeseman, J. R.; Keith, T.; Petersson, G. A.; Montgomery, J. A.; Raghavachari, K.; Al-Laham, M. A.; Zakrzewski, V. G.; Ortiz, J. V.; Foresman, J. B.; Cioslowski, J.; Stefanov, B. B.; Nanayakkara, A.; Challacombe, M.; Peng, C. Y.; Ayala, P. Y.; Chen, W.; Wong, M. W.; Andres, J. L.; Replogle, E. S.; Gomperts, R.; Martin, R. L.; Fox, D. J.; Binkley, J. S.; Defrees, D. J.; Baker, J.; Stewart, J. P.; Head-Gordon, M.; Gonzalez, C.; Pople, J. A. *GAUSSIAN 94*, Revision B.1; Gaussian, Inc.: Pittsburgh, PA, 1995.

(32) Deleuze, M. S.; Cederbaum, L. S. *J. Chem. Phys.* **1996**, *105*, 7583.

(33) Golod, A.; Deleuze, M.; Cederbaum, L. S. *J. Chem. Phys.* **1999**, *110*, 6014.

(34) Pang, W. N.; Gao, J. F.; Ruan, C. J.; Shang, R. C.; Trofimov, A. B.; Deleuze, M. S. *J. Chem. Phys.* **2000**, *108*, 8725.

(35) Deleuze, M. S.; Pang, W. N.; Salam, A.; Shang, R. C. *J. Am. Chem. Soc.* **2001**, *123*, 4049.

(36) (a) Bersuker, I. B. *The Jahn−Teller Effect and Vibronic Interactions in Modern Chemistry*; Plenum: New York, 1984. (b) Köppel, H.; Domcke, W.; Cederbaum, L. S. *Adv. Chem. Phys.* **1984**, *57*, 59.